Extension of Free-Surface Green's Function Multipole Expansion for Infinite Water Depth Case

B. Borgarino, A. Babarit, P. Ferrant

▶ **To cite this version:**

B. Borgarino, A. Babarit, P. Ferrant. Extension of Free-Surface Green's Function Multipole Expansion for Infinite Water Depth Case. International Journal of Offshore and Polar Engineering (IJOPE), 2011, 21 (3), pp.161-168. hal-01145111

HAL Id: hal-01145111
https://hal.science/hal-01145111

Submitted on 30 May 2019

HAL is a multi-disciplinary open access archive for the deposit and dissemination of scientific research documents, whether they are published or not. The documents may come from teaching and research institutions in France or abroad, or from public or private research centers.

L'archive ouverte pluridisciplinaire **HAL**, est destinée au dépôt et à la diffusion de documents scientifiques de niveau recherche, publiés ou non, émanant des établissements d'enseignement et de recherche français ou étrangers, des laboratoires publics ou privés.

Extension of the free-surface Green's function multipole expansion for the infinite water depth case

B. Borgarino, A. Babarit, P. Ferrant

Laboratoire de Mécanique des Fluides/EHGO (UMR CNRS 6598)
Ecole Centrale de Nantes,
Nantes, France

ABSTRACT

This paper presents new developments of the multipole expansion of the infinite water depth free-surface Green's function, in the scope of wave farm simulation. The expansions of the Green's function and its derivatives have been extended to be used in a 3D fast multipole algorithm. Previous restrictions over the use of the multipole expansion are proven to be unnecessary. Extensive validation is provided, by evaluating this function over a large range of parameters. The influence of the fast multipole algorithm parameters on the accuracy of the multipole expansion is then investigated.

KEY WORDS: free-surface Green's function; Boundary Element Method; Fast Multipole Method; multipole expansion; wave farm; Wave Energy Converters.

INTRODUCTION

Wave Energy Converters (WECs) are dedicated to be deployed in large arrays of typically 10 to 100 systems. An optimal spacing between the devices can help achieving the objectives of improving overall energy production and smoothing the overall power output. Simulation is necessary to determine how the farm should be organized and to investigate wake effects.

The resolution of the radiation/diffraction problems for a large array of systems using Boundary Element Methods (BEM) involves building and solving large, dense linear systems, requiring a $O(N^3)$ complexity. The challenge is to carry on each simulation fast enough to investigate different parameters in a reasonable amount of time: spacing between devices, wave parameters, bathymetry. A well-known solution for accelerating the BEM is the implementation of a General Minimum RESidual (GMRES) iterative solver, together with Fast Multipole Methods (FMM) for the fast calculation of matrix-vector products. This way the complexity can be reduced to $O(N)$.

The FMM is based on the multipole expansion of the free surface Green's function. For the constant depth case, the Green's function is described as series of terms containing the modified Bessel function of the second kind K_0 (Newman, 1985). Using Graf's addition theorem, the multipole expansion has been derived by (Utsunomiya and Watanabe, 2002). Combining this expansion and Higher Order Boundary Elements Method (HOBEM) and FMM, the hydrodynamic responses of a Very Large Floating Structure (VLFS) have been investigated. In (Teng and Gou, 2006), the results of the combination of the Constant Panel Method (CPM) or the HOBEM and the FMM are compared to analytical solutions for a floating box and a floating cylinder. In (Gou and Teng, 2008), the hydrodynamic interactions between three ships closely spaced have been studied.

Recently an expansion for the free-surface Green's function has been developed for the infinite water depth case (Utsunomiya and Okafuji, 2007), and applied to the case of a VLFS. This formulation is appropriate for describing a wave farm, which would ideally be situated in large depth, to avoid energy losses in the incident waves due to bathymetry effects. In case of shallow water, it is still possible to consider a complex seabed, represented as an independent, non-moving body.

The present paper is a continuation of this work: it extends the expansion formulation to make possible the use in a 3D FMM algorithm; the calculation of the normal derivatives of the Green function is described. The multipole expansion and the translation operators are extensively tested. The final objective here is to integrate these formulations and FMM in a in-house diffraction/radiation code, Aquaplus (Delhommeau, 1993).

FORMULATION

The boundary element problem

This section introduces the resolution of the diffraction/radiation problem by Aquaplus, based on BEM. The water is modeled as inviscid and incompressible. The fluid velocity is the gradient of a potential ϕ. The corresponding boundary problem is:

$$\Delta\phi = 0 \qquad \text{in the all fluid domain} \qquad (1)$$

$$\frac{\partial\phi}{\partial n} = 0 \qquad \text{on the seabed} \qquad (2)$$

$$\frac{\partial\phi}{\partial n} = \overrightarrow{V_i}.\overrightarrow{n} \qquad \text{on the surface } S_i \text{ of the body } i \qquad (3)$$

$$\frac{\partial^2\phi}{\partial t^2} + g\frac{\partial\phi}{\partial z} = 0 \qquad \text{on the free surface} \qquad (4)$$

Where g is the gravitation constant, $\overrightarrow{V}_i$ the velocity on the surface of the body i. Defining:

$$\Phi = Re[\phi e^{(-i\omega t)}] \tag{5}$$

$$\Phi(M) = \int\int_{S_i} \sigma(M').G(M,M')dS \tag{6}$$

and applying the second Green's formula leads to the integral equation:

$$\frac{\sigma(M)}{2} - \frac{1}{4\pi}\int\int_{S_i} \sigma(M')\frac{\partial G(M;M')}{\partial n}dS = \overrightarrow{V}_i.\overrightarrow{n}_{xyz} \tag{7}$$

With ω the wave pulsation, $\sigma(M)$ the source density at a point $M(x,y,z)$, assuming a source distribution. In the CPM, the surfaces of the bodies are discretized by N flat panels, where the unknowns σ are constant. (Eq. 7) has to be solved at the center of each panel, leading to a $N \times N$ linear system whose direct resolution requires a $O(N^3)$ complexity. Implementing an iterative solver accelerates the resolution; however it involves matrix-vector products $K.\sigma^{(l)}$ ($K_{ij} = \frac{\partial G(M_i;M_j)}{\partial n}$ and $\sigma_j^{(l)} = \sigma(M_j)$ evaluated at iteration (l), $i,j < N$). The contribution of the FMM to calculation speed-up is the direct evaluation of these products (each product requires a $O(N)$ complexity), without explicitly building K and σ.

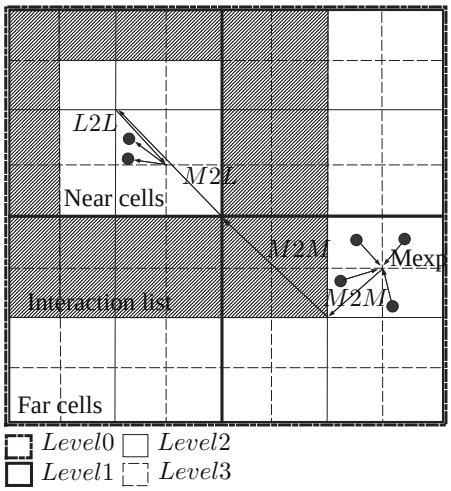

Fig. 1 – Principle of the FMM, illustrated in 2D

The Fast Multipole Method

The Fast Multipole Algorithm has been developed in (Greengard, 1988) to evaluate gravitational or electrostatic interactions in large systems of particles. (Liu and Nishimura, 2006) is a very clear introduction of the combination of BEM and FMM. Various versions of this algorithm are described in (Carrier et al., 1988), (Cheng et al., 1999).

The FMM decomposes the physical space in "cells", using a hierarchical oct-tree. A cell is a cube containing one or more panels (≈ 10). Instead of direct panel-to-panel interactions, the FMM computes the interaction between groups of panels sufficiently far from each other. The discrimination between "far" and "near" depends on the relative position of the cells. The influence of a group of panel is evaluated by calculating and summing together the moments of the multipole expansion of $\left(\sigma.\frac{\partial G}{\partial n}\right)$ for each panel (Eq. 38). Then this influence is displaced to the target cell thanks to translation operators, and added to contributions from other groups of panels. The sum of contributions is then "spread" on the panels of the influenced cell. This corresponds to the double integral in (Eq. 7), but applied only on the surface defined by panels far enough from the influenced panel. Closer interactions are calculated by the direct method and added to the previous result.Translation operators depend on the relationship between the cells:

– Moment to Moment (M2M): from the child cell center to the parent cell center
– Moment to Local (M2L): from parent to child or between two sibling cell (converts a multipole expansion into a Taylor expansion)
– Local to Local (L2L): from parent to child

(Fig. 1) shows the hierarchical decomposition of a 2D space. $Level1$ cells are children of the $Level0$ cell, and so on. The different steps to transpose the influence of four panels of far cells to two panels of the target cell are represented ($Mexp$ is the multipole expansion).

The free surface Green's function

In (Utsunomiya and Okafuji, 2007), the Green's function follows the integral form described in (Newman, 1985):

$$G(x,y,z;\xi,\eta,\zeta) = \frac{1}{r} + \frac{1}{r_1} + \int_0^\infty \frac{2\nu}{k-\nu}e^{k(z+\zeta)}J_0(kR)dk \tag{8}$$

With :
(ξ,η,ζ) coordinates of the source point S (influencing point)
(x,y,z) coordinates of the field point F (influenced point)
ν the wave number
J_n the n^{th} order Bessel function of the first kind
$r = \sqrt{(x-\xi)^2+(y-\eta)^2+(z-\zeta)^2}$
$r_1 = \sqrt{(x-\xi)^2+(y-\eta)^2+(z+\zeta)^2}$
$R = \sqrt{(x-\xi)^2+(y-\eta)^2}$
The coordinate of S and F are $S(r_\xi,\alpha_\xi,\theta_\xi)$ and $F(r_x,\alpha_x,\theta_x)$ in the spherical system, and $S(R_\xi,\alpha_\xi,\zeta)$ and $F(R_x,\alpha_x,z)$ in the cylindrical system, both systems centered in $G(x_G,y_G,0)$. Considering Lipschitz's integral:

$$\frac{1}{r_1} = \int_0^\infty e^{k(z+\zeta)}J_0(kR)dk \tag{9}$$

We have :

$$G(x,y,z;\xi,\eta,\zeta) = \frac{1}{r} - \frac{1}{r_1} + \int_0^\infty \frac{2k}{k-\nu}e^{k(z+\zeta)}J_0(kR)dk \tag{10}$$

This paper is based on (Eq. 10), which is the formulation originally implemented in Aquaplus.

MULTIPOLE EXPANSION

This section develops the multipole expansion of the Green's function following the demonstration of (Utsunomiya and Okafuji, 2007). We show that restrictions present in this reference for the near field are not necessary.

Graf's addition theorem

This theorem (Watson, 1944) is the base for the multipole expansion of the Green's function and its translation operators. Let's consider the triangle on (Fig. 2) such that $Z - zcos\alpha = wcos\beta$ and $zsin\alpha = wsin\beta$. Then:

$$J_\nu(w)e^{i\nu\beta} = \sum_{m=-\infty}^{\infty} J_{m+\nu}(Z)J_m(z)e^{im\alpha} \tag{11}$$

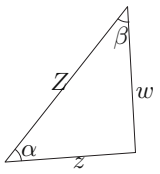

Fig. 2 – Addition theorem of the Bessel functions

Near field

G_1 represents the near field :

$$G_1 = \frac{1}{r} - \frac{1}{r_1} \tag{12}$$

According to Lipschitz's integral, we have:

$$\frac{1}{r} = \int_0^\infty e^{-k|z-\zeta|} J_0(kR) dk \tag{13}$$

In (Utsunomiya and Okafuji, 2007), only the case $z < \zeta$ is studied, making the expansion of G_1 only valid when the source point is above the field point. $\frac{1}{r}$ being symmetrical, we demonstrate here the following expansion for the case $\zeta < z$:

$$G_1 = \int_0^\infty e^{k\zeta}(e^{-kz} - e^{kz}) J_0(kR) dk \tag{14}$$

(Eq. 11) is applied in the triangle defined by S, F and G (center of the multipole expansion) seen from above such that $w = R$, $Z = R_x$, $z = R_\xi$ and $\alpha = \alpha_x - \alpha_\xi$. Then:

$$G_1 = \int_0^\infty e^{k\zeta}(e^{-kz} - e^{kz}) \sum_{m=-\infty}^{\infty} J_m(kR_x) e^{im\alpha_x} J_m(kR_\zeta) e^{-im\alpha_\zeta} dk \tag{15}$$

According to (Utsunomiya and Okafuji, 2007), for $\zeta < 0$,

$$e^{k\zeta} J_m(kR_\xi) = \epsilon_m \sum_{n=|m|}^{\infty} (r_\xi)^n \frac{P_n^{|m|}(cos\theta_\xi)}{(n+|m|)!} k^n \tag{16}$$

$$e^{-k\zeta} J_m(kR_\xi) = \epsilon_m \sum_{n=|m|}^{\infty} (-1)^{n+m} (r_\xi)^n \frac{P_n^{|m|}(cos\theta_\xi)}{(n+|m|)!} k^n \tag{17}$$

With:

$$\epsilon_m = \begin{cases} 1 & \text{if} \quad m \geq 0 \\ (-1)^m & \text{if} \quad m < 0 \end{cases} \tag{18}$$

The P_n^m terms are Legendre associated functions, defined in Thorne's sense, i.e to a factor $(-1)^m$ compared to the usual definition. Referring to (Gray and Mathews, 1922), Utsunomiya derives the following expression $\forall m$, $z < 0$:

$$\int_0^\infty e^{kz} J_m(kR_x) k^n dk = \epsilon_m (-1)^{n+m} (n-|m|)! \frac{P_n^{|m|}(cos\theta_x)}{r_x^{n+1}} \tag{19}$$

noting that:

$$P_n^{|m|}(-cos\theta_x) = (-1)^{m+n} P_n^{|m|}(cos\theta_x) \tag{20}$$

leads to the modification of (Eq. 19), changing z into $-z$ (i.e $z > 0$):

$$\int_0^\infty e^{kz} J_m(kR_x) k^n dk = \epsilon_m (n-|m|)! \frac{P_n^{|m|}(cos\theta_x)}{r_x^{n+1}} \tag{21}$$

If we note that:

$$\sum_{m=-\infty}^{\infty} \sum_{n=|m|}^{\infty} = \sum_{n=0}^{\infty} \sum_{m=-n}^{n} \tag{22}$$

and that $\epsilon_m \times \epsilon_m = 1$, substituting (Eqs. 16, 19, 21) in (Eq. 15) gives the multipole expansion of G_1:

$$\begin{aligned} G_1 = \sum_{n=0}^{\infty} \sum_{m=-n}^{n} [-(-1)^{n+m} + 1] r_\xi^n \frac{P_n^{|m|}(cos\theta_\xi)}{(n+|m|)!} e^{-im\alpha_\xi} \\ e^{im\alpha_x} (n-|m|)! \frac{P_n^{|m|}(cos\theta_x)}{r_x^{n+1}} \end{aligned} \tag{23}$$

The formulation in (Utsunomiya and Okafuji, 2007) for $z < \zeta$ and (Eq. 23) are the same, except the minus sign in $[-(-1)^{n+m} + 1]$ due to the original definition of G_1 (Eq. 12). Then no restriction on the relative vertical position of the source and field points has to be applied.
This multipole expansion is an infinite sum of terms. Numerically it has to be truncated. To obtain a satisfying accuracy, the quantity $\left(\frac{r_\xi}{r_x}\right)^n$ has to be as small as possible, i.e the source point has to be close enough to the expansion center.

Far field

The far field part of the Green's function is defined by:

$$G_2 = \int_0^\infty \frac{2k}{k-\nu} e^{k(z+\zeta)} J_0(kR) dk \tag{24}$$

Using the same equations as previously leads to the multipole expansion of G_2:

$$G_2 = 2 \sum_{n=0}^{\infty} \sum_{m=-n}^{n} r_\xi^n \frac{P_n^{|m|}(cos\theta_\xi)}{(n+|m|)!} e^{-im\alpha_\xi} e^{im\alpha_x} G_3' \tag{25}$$

with:

$$G_3' = \int_0^\infty \frac{k}{k-\nu} e^{-k|z|} J_{|m|}(kR_x) k^n dk \tag{26}$$

$$\begin{aligned} G_3' = \int_0^\infty \frac{k-\nu}{k-\nu} e^{kz} J_{|m|}(kR_x) k^n dk \\ + \nu \int_0^\infty \frac{1}{k-\nu} e^{kz} J_{|m|}(kR_x) k^n dk \end{aligned} \tag{27}$$

$$G_3' = (-1)^{m+n-1} (n-1-|m|)! \frac{P_{n-p}^{|m|}(cos\theta_x)}{r_x^n} + \nu G_3 \tag{28}$$

G_3 is defined in (Utsunomiya and Okafuji, 2007) by:

$$G_3 = \int_0^\infty \frac{1}{k-\nu} e^{kz} J_{|m|}(kR_x) k^n dk \tag{29}$$

$$G_3 = \begin{cases} \sum_{p=1}^{n-|m|} \nu^{p-1} (-1)^{m+n-p} (n-p-|m|)! \frac{P_{n-p}^{|m|}(cos\theta_x)}{r_x^{n-p+1}} \\ +\nu^{n-|m|} \int_0^\infty \frac{1}{k-\nu} e^{kz} J_{|m|}(kR_x) k^{|m|} dk \ \text{ if } n > |m| \\ \\ \int_0^\infty \frac{1}{k-\nu} e^{kz} J_{|m|}(kR_x) k^{|m|} dk \ \text{ if } n = |m| \end{cases} \tag{30}$$

in which the last integral defined as G_4 can be evaluated by (Eq. 31), for $m > 0$:

$$G_4 = \frac{2}{\pi}\Big(\frac{-\nu^m\pi^2 e^{kz}}{4}[(-1)^m\mathbf{H}_{-\mathbf{m}}(\nu R_x) - Y_m(\nu R_x)] + \frac{\sqrt{\pi}(2R_x)^m\Gamma(m+\frac{1}{2})}{2}\int_0^z \frac{e^{\nu(z-s)}}{(s^2+R_x^2)^{m+\frac{1}{2}}}ds\Big) - \pi\nu^m i e^{\nu z}H_m^{(2)}(\nu R_x) \quad (31)$$

with $\mathbf{H}$ the Struve function, $H^{(2)}$ the second kind Hankel function, Y the second kind Bessel function, and Γ the Gamma function. Note that:

$$Im(G_2) = -2\pi\sum_{n=0}^{\infty}\sum_{m=-n}^{n}(\nu r_\xi)^n\frac{P_n^{|m|}(cos\theta_\xi)}{(n+|m|)!}e^{-im\alpha_\xi}e^{\nu z}J_m(R_x)e^{im\alpha_x} \quad (32)$$

In (Eq. 32), the term $(\nu r_\xi)^n$ has to be as small as possible to get a good convergence of the expansion of $Im(G_2)$.

CENTER OF EXPANSION OUT OF THE FREE SURFACE

In (Utsunomiya and Okafuji, 2007) the center of the multipole expansion is located on the free-surface and the translation operations are calculated along this surface. Indeed, the problem studied (a Very Long Floating Structure) has small vertical dimensions compared to horizontal, and is probably seen as a 2D problem. The resolution on the free surface uses a 2D fast multipole algorithm.
In the case of wave farm, the studied bodies have equivalent vertical and horizontal dimensions. Plus, the study of the bathymetry will lead to non-negligible vertical dimensions. This makes necessary to use a 3D fast multipole algorithm in which the multipole expansion can be done anywhere in the fluid domain.

Far field

The product under the integral of G_2 (Eq. 24) can be split in two different ways:

$$e^{k(z+\zeta)}J_0(kR) = \sum_{m=-\infty}^{m=\infty} e^{k(\zeta-z_G)}J_m(kR_\xi)e^{k(z+z_G)}J_m(kR_x) \quad (33)$$

$$= \sum_{m=-\infty}^{m=\infty} e^{k(\zeta+z_G)}J_m(kR_\xi)e^{k(z-z_G)}J_m(kR_x) \quad (34)$$

with $G(x_G, y_G, z_G)$ the center of the multipole expansion ($z_G \leq 0$) and $R_x > R_\xi$. Considering that the center of the expansion has to be relatively close to the source point, only (Eq. 33) will lead to a valid expansion, see (Fig. 3). Following the same demonstration steps than previously leads to:

$$G_2 = 2\sum_{n=0}^{\infty}\sum_{m=-n}^{n} r_\xi^n\frac{P_n^{|m|}(cos\theta_\xi)}{(n+|m|)!}e^{-im\alpha_\xi}G_3'(z_x', R_x')e^{im\alpha_x'} \quad (35)$$

Here the coordinates of the source point $S(r_\xi, \theta_\xi, \alpha_\xi)$ are now expressed in the system centered in $G(x_G, y_G, z_G)$ and the coordinates of the source field $S(r_x', \theta_x', \alpha_x')$ in the system centered in $G'(x_G, y_G, -z_G)$. See an example on (Fig. 3), noting that $\alpha_x' = \alpha_x$ and $R_x' = R_x$.

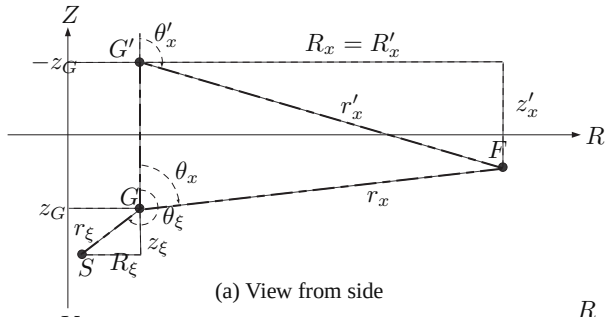

(a) View from side

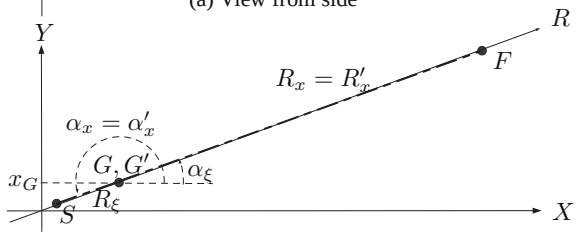

(b) View from above

Fig. 3 – Coordinate systems in use for $z_G \neq 0$ (simplified case with S, G and F aligned)

Near field

For G_1, supposing $\zeta - z < 0$:

$$G_1 = \int_0^\infty \sum_{m=-\infty}^{\infty} \underbrace{e^{k(\zeta-z_G)}J_m(kR_\xi)}_{(1)}e^{-im\alpha_\xi} (\underbrace{e^{-k(z-z_G)}J_m(kR_x)}_{(2)} - \underbrace{e^{k(z+z_G)}J_m(kR_x)}_{(3)})e^{im\alpha_x}dk \quad (36)$$

$z + z_G$ is negative, we use (Eq. 19) to calculated (3)'s contribution to the expansion. Given that G is close to S, $z_G \approx \zeta$, $-(z - z_G)$ is positive and (Eq. 21) is used for (2). $\zeta - z_G$ in (1) can be positive or negative, but (Eq. 16) is used for any case:
– if negative, (Eq. 16) directly applies
– if positive, then $z_G - \zeta < 0$. We apply (Eq. 16) to $e^{-k(z_G-\zeta)}J_m(kR_\xi)$, which mean expressing the position of G in a coordinates system centered in S and changes $cos\theta_\xi$ in $cos(\theta_\xi+\pi) = -cos\theta_\xi$. Using (Eq. 20), we get back to (Eq. 16).
This eventually gives the following multipole expansion:

$$G_1 = \sum_{n=0}^{\infty}\sum_{m=-n}^{n} r_\xi^n\frac{P_n^{|m|}(cos\theta_\xi)}{(n+|m|)!}e^{-im\alpha_\xi} e^{im\alpha_x'}(n-|m|)!\left(\frac{P_n^{|m|}cos\theta_x}{r_x^{n+1}} - (-1)^{n+m}\frac{P_n^{|m|}cos\theta_{x'}}{r_{x'}^{n+1}}\right) \quad (37)$$

The coordinate of the field point are (r, α_x, θ_x) in the system centered in G, and $(r', \alpha_x', \theta_x')$ in the system centered in G'. The same expression can be demonstrated for the case $\zeta - z > 0$. As a consequence, there is no restriction on the relative vertical positioning of S, F, G.
The term related to the source point appearing in G_1 and G_2 is called

the moment of the multipole expansion:

$$M_n^m = r_\xi^n \frac{P_n^{|m|}(cos\theta_\xi)}{(n+|m|)!} e^{-im\alpha_\xi} \tag{38}$$

NORMAL DERIVATIVES

The integral equations traducing in the diffraction/radiation problem involves the normal derivatives of the Green's function, calculated at the source point. According to (Utsunomiya and Watanabe, 2002), the normal derivatives of the Green's function at the source point can be obtained from the gradient of the moments:

$$\overrightarrow{grad}\, M_n^m = \frac{\partial M_n^m}{\partial r}\overrightarrow{e_r} + \frac{1}{r}\frac{\partial M_n^m}{\partial \theta}\overrightarrow{e_\theta} + \frac{1}{r sin\theta}\frac{\partial M_n^m}{\partial \alpha}\overrightarrow{e_\alpha} \tag{39}$$

with $(\overrightarrow{e_r}, \overrightarrow{e_\theta}, \overrightarrow{e_\alpha})$ the orthonormal base of the spherical system centered in $(x_G, y_G, 0)$. Referring to (Eq. 38), the partial derivative in relation to α and r are trivial when $z_G = 0$. Derivatives related to θ call the derivative of P_n^m (obtained by recurrence relationships, as well as P_n^m). For $z_G \neq 0$, one needs to compose the derivatives in order to calculate the gradient at the source point $S(r_R, \alpha_\xi, \theta_R)$, see (Fig. 4).

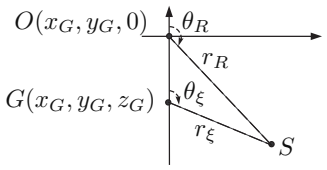

Fig. 4 – Coordinate systems when $zG \neq 0$

It leads to :

$$\frac{\partial}{\partial \alpha_R} M_n^m = \frac{\partial}{\partial \alpha_\xi} M_n^m = -im(r_\xi^n)\frac{P_n^{|m|}(cos\theta_\xi)}{(n+|m|)!} e^{-im\alpha_\xi} \tag{40}$$

$$\begin{aligned}\frac{\partial}{\partial r_R} M_n^m = [r_\xi^n \frac{\partial cos\theta_\xi}{\partial r_R}\frac{\partial P_n^{|m|}(cos\theta_\xi)}{\partial cos\theta_\xi} \\ + P_n^{|m|}(cos\theta_\xi)\frac{\partial r_\xi}{\partial r_R} n\, r_\xi^{n-1}]\frac{e^{-im\alpha_\xi}}{(n+m)!}\end{aligned} \tag{41}$$

$$\begin{aligned}\frac{\partial}{\partial \theta_R} M_n^m = [r_\xi^n \frac{\partial cos\theta_\xi}{\partial \theta_R}\frac{\partial P_n^{|m|}(cos\theta_\xi)}{\partial cos\theta_\xi} \\ + P_n^{|m|}(cos\theta_\xi)\frac{\partial r_\xi^n}{\partial \theta_R}]\frac{e^{-im\alpha_\xi}}{(n+m)!}\end{aligned} \tag{42}$$

With:

$$\frac{\partial r_\xi}{\partial r_R} = \frac{r_R - z_G\, cos\theta_R}{\sqrt{r_R^2 + z_G^2 - 2\, z_G\, r_R cos\theta_R}} \tag{43}$$

$$\frac{\partial cos\theta_\xi}{\partial r_R} = \frac{z_G}{r_R^2}\frac{sin\theta_\xi}{sin\theta_R}\frac{1}{1 + \frac{cos^2\theta_\xi}{sin^2\theta_R}} \tag{44}$$

$$\frac{\partial cos\theta_\xi}{\partial \theta_R} = -sin\theta_R \frac{sin\theta_\xi + cos\theta_\xi \frac{cos\theta_R}{sin\theta_R}}{sin\theta_R + \frac{cos\theta_\xi}{sin\theta_\xi}(cos\theta_R - \frac{z_G}{r_R})} \tag{45}$$

$$\frac{\partial r_\xi^n}{\partial \theta_R} = sin\theta_R (r_R^2 + z_G^2 + 2 z_G r_R cos\theta_R)^{\frac{n}{2}-1} \tag{46}$$

TRANSLATION OPERATORS

The expressions of the moments obtained by M2L and L2L are based on the splitting of the moments of the multipole expansion, using (Eq. 11). They have not been changed compared to (Utsunomiya and Okafuji, 2007) by $z_G \neq 0$:

$$\tilde{M}_n^m = \sum_{t=0}^{n}\sum_{s=-t}^{t} M_{n-t}^{m-s}\epsilon_{m-s}\epsilon_s\epsilon_m r_{x_M}^t \frac{P_t^{|s|}(cos\theta_{x_M})}{(t+|s|)!} e^{-is\alpha_{x_M}} \tag{47}$$

$$\begin{aligned}\tilde{L}_u^{v(1)(2)} = \sum_{t=v}^{\infty}\sum_{s=-t}^{t} \frac{\epsilon_{u-s}\epsilon_u}{\epsilon_s} L_t^s (-1)^{(t-v)+(u-s)} r_{x_L}^{t-v} \\ \frac{P_{t-v}^{u-s}(cos\theta_{x_L})}{[(t-v)-|u-s|]!} e^{-i(u-s)\alpha_{x_L}}\end{aligned} \tag{48}$$

With M and $L^{(1)(2)}$ the original multipole and local expansion coefficients, $\tilde{M}$ and $\tilde{L}^{(1)(2)}$ the translated ones, $(r_{x_M}, \alpha_{x_M}, \theta_{x_M})$ the position of the original expansion center seen from the new one (for the M2L), and $(r_{x_L}, \alpha_{x_L}, \theta_{x_L})$ the position of the local expansion center seen from the new one (for the L2L).

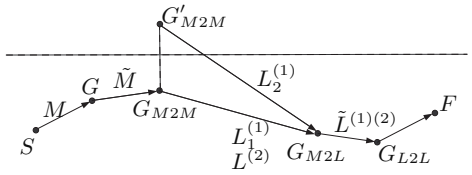

Fig. 5 – Moments of the expansion depending on the translation (operators identified by the $G_{...}$ they point to)

As shows (Fig. 5), the M2L for $L^{(1)}$ depends on the original center of expansion (here G_{M2M}) and on its symmetrical in relation to the free-surface G'_{M2M}. The translation operator can be found by applying (Eq. 11) to the Bessel function in G'_3 (Eq. 35), using the following horizontal triangle:

– $w = R_x$, $Z = R_{x_{ML}}$ and $z = R_{F_{ML}}$
– $\beta = \alpha_x - (\alpha_{x_{ML}} - \pi)$ and $\alpha = \alpha_{x_{ML}} - \alpha_{F_{ML}}$

with

– the coordinates of the center of the multipole expansion and its symmetrical seen from the local expansion point are subscripted by x_{ML} and x'_{ML}
– the coordinates of F seen from the local expansion point are subscripted by F_{ML}

Referring to (Eq. 37),

$$L_t^{s(1)} = \sum_{n=0}^{\infty}\sum_{m=-n}^{n} {L_1^{(1)}}_n^m + {L_1^{(2)}}_n^m \tag{49}$$

$$L_t^{s(1)} = \sum_{n=0}^{\infty} \sum_{m=-n}^{n} \epsilon_{m-s}\epsilon_s\epsilon_m M_n^m[(n+t)-|s-m|]! \left(\frac{P_{n+t}^{|s-m|}(cos\theta_{x_{ML}})}{{r_{x_{ML}}}^{n+t+1}}(-1)^{n-m} - \frac{P_{n+t}^{|s-m|}(cos\theta_{x'_{ML}})}{r_{x'_{ML}}^{n+t+1}} \right) e^{-i(s-m)\alpha_{x_{ML}}} \quad (50)$$

The calculation of $L^{(2)}$ remains unchanged:

$$L_t^{s(2)} = \sum_{n=0}^{\infty} \sum_{m=-n}^{n} \epsilon_{m-s}\epsilon_s\epsilon_m M_n^m[(n+t)-|s-m|]! \; e^{-i(s-m)\alpha_{x_{ML}}} \int_0^{\infty} \frac{k}{k-\nu} e^{-k|z_{x_{ML}}|} J_{|s-m|}(kR_{x_{ML}}) k^{n+t} dk \quad (51)$$

Finally the evaluation of G_1 and G_2 is given by:

$$G_{(1)(2)} = \sum_{v=0}^{\infty} \sum_{u=-v}^{v} \tilde{L}_v^{u(1)(2)} (r_x)^v \frac{P_v^{|u|}(cos\theta_x)}{(v+|u|)!} e^{iu\alpha_x} \quad (52)$$

with $(r_x, \alpha_x, \theta_x)$ the coordinate of the field point seen from the local expansion center and the local moments $\tilde{L}_v^{u(1)(2)}$ defined in (Eq. 48). Note that the local moments are different for G_1 and G_2.

NUMERICAL VALIDATION

The multipole expansion of the Green's function and its derivatives have been implemented in Fortran routines, as well as translation operators. The calculation of special functions is made by routines from (Jin, 1996).

General verification

The Green's function and its derivatives have been calculated between the source point S and the field point F. Direct calculations have been performed, as well as calculations with several intermediary points, enabling the use of the translation operators. For each calculation, the following parameters can vary:

- wave number ν, calculated for periods from 3 s to 20 s
- the horizontal distance R between S and F, from 15 m to 150 m
- the vertical distance Z between S and F, from 5 m to 55 m

Two types of test have to be carried on, G_2 being non symmetrical:

- Test 1: S close to the free surface, the horizontal and vertical coordinates of F varying
- Test 2: the depth of S varying, F close to the free-surface with only its horizontal coordinate varying

Inside each series of tests the relative position $\overrightarrow{SG}$ have been kept the same to have $r_\xi << r_x$. Different series have been studied, with different positioning: $\zeta < z_G$, $\zeta > z_G$. The order of the expansion Np is 12. The Green's function (and derivatives) can be plotted on non-dimensional maps $(\nu R, \nu z)$ such as (Figures 6,7,8), which gather more than 23,000 evaluations. The color layers are obtained by triangulation, what explains the non-smooth aspect of certain plots.

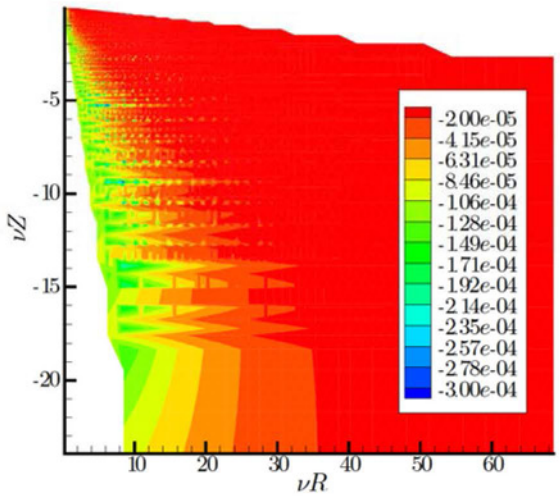

Fig. 6 – G_1 (m^{-1})

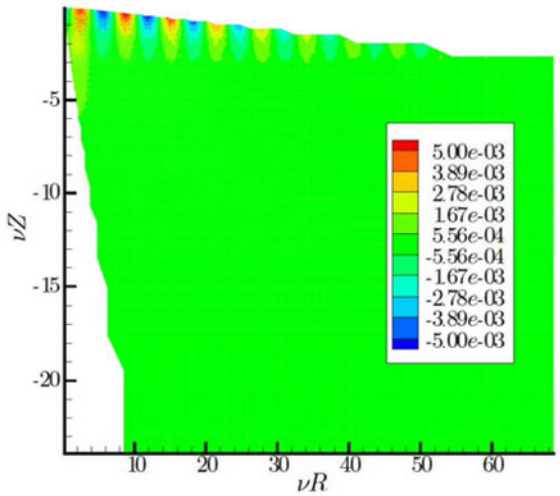

Fig. 7 – $Re(G_2)$ (m^{-1})

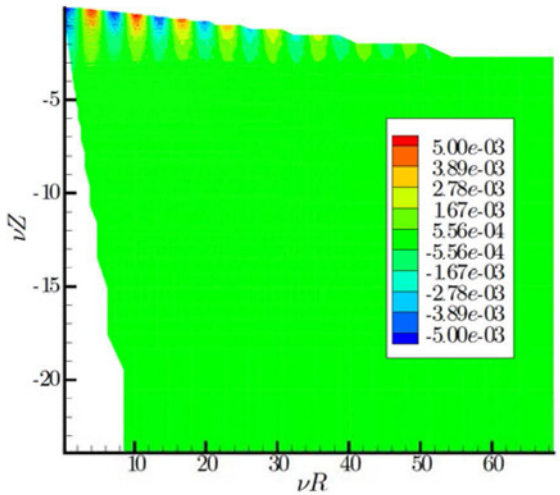

Fig. 8 – $Im(G_2)$ (m^{-1})

These plots can be compared to results from Aquaplus. It shows a relatively good agreement (Tab. 1). However, a better accuracy is found by

comparing the multipole results to analytical solutions: G_1 is given by (Eq. 12), and from (Wehausen and Laitone, 1960), we have:

$$Im(G_2) = 2\pi e^{\nu(\zeta+z)} J_0(\nu R) \tag{53}$$

$$\lim_{r\to+\infty} G_1 + Re(G_2) = -2\pi e^{\nu(\zeta+z)} Y_0(\nu R) \tag{54}$$

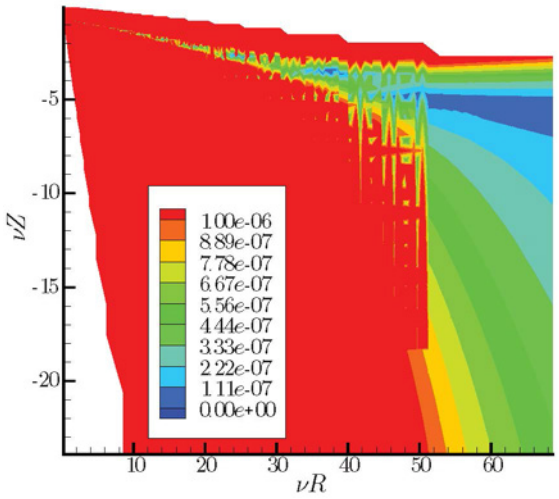

Fig. 9 – Absolute difference between $G_1 + Re(G_2)$ calculated by multipole expansion and Eq. 54

The asymptotic behavior of $G_1 + Re(G_2)$ is clearly outlined, see (Fig. 9). Tab. 1 shows that the results from the multipole expansion agree best with the analytical solutions than with Aquaplus, suggesting that they might be more precise. When no analytical result is available, a general good agreement with Aquaplus is found, which is comforting in the scope of the implementation of FMM in the code. Parameters of the FMM such as the order of the expansion and the relative positioning of S, G and F which influence the accuracy of the expansion are investigated in next section.

Tab. 1 – Maximum error (m^{-1}) on the multipole expansion of the Green's function over the $(\nu R, \nu Z)$ domain

Multipole compared to ...	Aquaplus	Analytical
G_1	3.10^{-10}	2.10^{-10}
$Re(G_2)$	2.10^{-4}	X
$Im(G_2)$	9.10^{-5}	6.10^{-9}

Position of the expansion center

In order to have global accuracy indicators, we calculate the average and the maximum values of the relative error over the domain $(\nu R, \nu Z)$, between the multipole expansion and the analytical value of G_1 and $Im(G_2)$. This way we investigate the influence of:
– the expansion order Np
– the ratio $\mathbf{r}_{G_1} = \frac{r_\xi}{r_x}$ on G_1
– the ratio $\mathbf{r}_{G_2} = \frac{r_\xi}{\lambda} = \nu r_\xi$ on $Im(G_2)$
(Figures 10,11) have been obtained by tests of the type "Test 2", the position of G depending on the distance (SF) through $\mathbf{r}_{G_1}$ and $\mathbf{r}_{G_2}$. This do not pretend to be an exhaustive study, but gives an idea of the influence of FMM parameters.
As expected the overall accuracy gets better with an increasing Np and decreasing $\mathbf{r}_{G_1}$ and $\mathbf{r}_{G_2}$. An order smaller than 4 has to be avoided. A large order gives a good precision on a large range of values for $\mathbf{r}_{G_1}$ and $\mathbf{r}_{G_2}$. $Np \approx 8$ seems to be a good compromise, as stated in (Board et al., 1995).

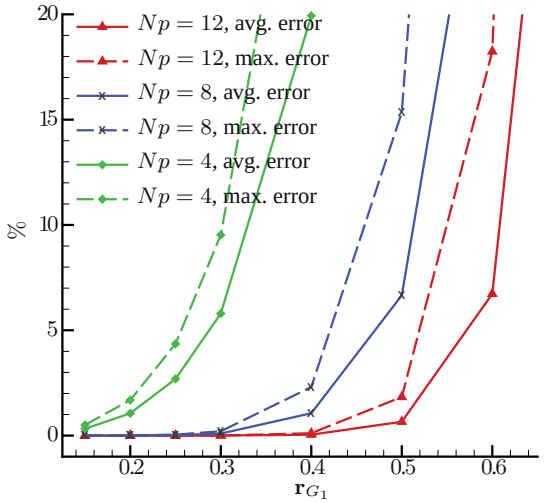

Fig. 10 – Average and maximum relative error on G_1, depending on Np and $\mathbf{r}_{G_1}$

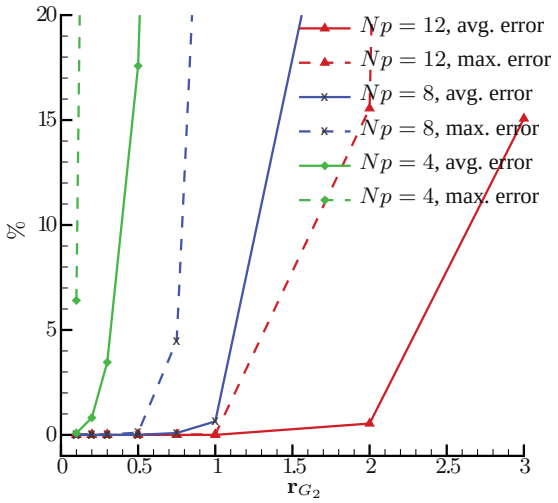

Fig. 11 – Average and maximum relative error on $Im(G_2)$, depending on Np and $\mathbf{r}_{G_2}$

From these results, characteristic parameters of the Fast Multipole Algorithm can be estimated, for a required Np and precision. For instance, considering $Np = 8$, it seems reasonable to work with:

$$\begin{cases} \mathbf{r}_{G_1} \leq 0.3 \\ \mathbf{r}_{G_2} \leq 1 \end{cases} \tag{55}$$

On the other hand, considering the original FMM (Greengard, 1988),

$$\begin{cases} r_\xi \leq \frac{\sqrt{3}}{2}a & \text{(expansion calculated at the center of the parent cell)} \\ r_x \geq 2a & \text{(cells well separated are at least } 2a \text{ distant)} \end{cases} \tag{56}$$

with a the cell side size. It leads to:

$$\mathbf{r}_{G_1} \leq 0.43 \tag{57}$$

more or less the same range of $\mathbf{r}_{G_1}$ than in (Eq. 55). From the second condition in (Eq. 55), and from (Eq. 56), we have a condition on the cell size:

$$a = \frac{2 \times 1.0}{\nu\sqrt{3}} = 1.15\lambda \tag{58}$$

From the hierarchical decomposition of space in the FMM,

$$a = \frac{L_{max}}{2^{N_L}} \tag{59}$$

with L_{max} the maximum dimension of the system and N_L the number of levels in the FMM. We eventually get:

$$N_L = log\left(\frac{L_{max}}{1.15\lambda}\right) \tag{60}$$

Referring to the VLFS studied in (Utsunomiya and Okafuji, 2007) with the same multipole expansion, $L_{max} = 2000m$, $\lambda = 100m$, corresponding to 5 levels. For smaller periods (3 s) and a $90m \times 90m$ problem (DNV barge, (Delhommeau, 1993)), 5 levels are necessary. These values are sensible, but for a 1-square-km wave farm N_L would increase up to 9, maybe leading to computational difficulties. This problem is rather new, as we study the behavior and interactions of systems possibly sensitive to small wave lengths over a large distance.

CONCLUSIONS

The extension of the multipole expansion of the free-surface Green's function for the infinite water depth case permits to apply it to a wider range of situations. Restriction on the relative positions between interacting points have been canceled. The expansion and the FMM translation operators have been evaluated at any depth, enabling the future use of a 3D FMM algorithm. The expansion of the Green's function, of its derivatives and the translation operators have been extensively tested.

The accuracy of the developed formulations have been partially investigated for the far field when analytical results were available for comparison, i.e for the Rankin singularity of the Green's function as well as for its oscillatory part. This investigation gives an order of magnitude of the accuracy when computing the Green's function, depending on the Fast Multipole MEthod parameters.

The next step is to implement the FMM based on these formulations in the diffraction/radiation code Aquaplus. An open-source fast multipole algorithm, the Distributed Parallel Multipole Tree Algorithm (DPMTA) (Rankin, 1999) is currently being adapted at the LMF in this scope.

ACKNOWLEDGMENTS

The authors would like to acknowledge ADEME (the French environment agency) and Région Pays de la Loire for funding the Phd program in which this study has been done.

REFERENCES

Board, J. A., Hakura, Z. S., Elliot, W. D., and Rankin, W. T. (1995). Scalable variants of multipole-accelerated algorithms for molecular dynamics applications. Technical report, Duke University, Department of Electrical Engineering.

Carrier, J., Greengard, L., and Rokhlin, V. (1988). A fast adaptative multipole algorithm for particles simulation. *Journal on scientific computing*, 9.

Cheng, H., Greengard, L., and Rokhlin, V. (1999). A fast adaptative multipole algorithm in three dimensions. *Journal of Computational Physics*, 155:468–498.

Delhommeau, G. (1993). Seakeeping codes aquadyn and aquaplus. In *19th WEGMENT School, Numerical Simulation of Hydrodynamics: Ship and Offshore Structures*.

Gou, Y. and Teng, B. (2008). Research on hydrodynamic interaction between multiple floating bodies. Technical report, State Key Laboratory of Coastal and Offshore Engineering, Dalian University of Technology.

Gray, A. and Mathews, G. (1922). *A Treatise on Bessel Functions and Their Applications to Physics*. Macmillan, London.

Greengard, L. (1988). *The Rapid Evaluation of Potential Fields in Particle Systems*. MIT Press.

Jin, J. (1996). Fortran routines for computation of special functions.

Liu, Y. J. and Nishimura, N. (2006). The fast multipole boundary element method for potential problems: A tutorial. *Engineering Analysis with Boundary Elements*, 30:371–381.

Newman, J. N. (1985). Algorithms for free-surface green's function. *Journal of engineering mathematics*, 19:57–67.

Rankin, W. T. (1999). *Efficient Parallel Implementations of Multipole Based N-Body Algorithms*. PhD thesis, Department of Electrical Engineering, Duke University.

Teng, B. and Gou, Y. (2006). Fast multipole expansion method and its application in bem for wave diffraction and radiation. In *Proc. 16th International Offshore and Polar Engineering Conference, San Fransisco, California*.

Utsunomiya, T. and Okafuji, T. (2007). Wave response of a vlfs by accelerated green's fucntion method in infinite water depth. *International Journal of Offshore and Polar Engineers*, 17:30–38.

Utsunomiya, T. and Watanabe, E. (2002). Accelerated higher order boundary element method for wave diffraction/radiation problems and its applications. In *Proc. 12 th International Offshore and Polar Engineering Conference, Kitakyushu, Japan*.

Watson, G. N. (1944). *A treatise on the theory of Bessel functions*. Cambridge University Presse.

Wehausen, J. V. and Laitone, E. V. (1960). *Surface Waves*, chapter Sec. 13. Springer Verlag.